Scilight

Applied Mathematics and Statistics
https://www.sciltp.com/journals/ams

Article

Check for updates

Mathematical Model of Co-Infection of Malaria and COVID-19 in Malaria-Endemic Population

Michael C. Anyanwu * and Emmanuel C. Duru

Department of Mathematics, Michael Okpara University of Agriculture, Umudike 440101, Nigeria
* Correspondence: anyanwu.michael@mouau.edu.ng

How To Cite: Anyanwu, M.C.; Duru, E.C. Mathematical Model of Co-Infection of Malaria and COVID-19 in Malaria-Endemic Population. *Applied Mathematics and Statistics* **2026**, *3*(2), 18. https://doi.org/10.53941/ams.2026.100018

Received: 26 June 2026
Revised: 14 August 2026
Accepted: 24 August 2026
Published: 4 September 2026

Abstract: Malaria and coronavirus disease (COVID-19) have been shown to exhibit clinical and pathological resemblances. The overlap in their characteristic symptoms led to the loss of many lives during the COVID-19 pandemic due to misdiagnosis and wrong treatment. In this paper, co-circulation and co-infection of malaria and coronavirus disease in a malaria-endemic population are modeled through a system of nonlinear ordinary differential equations, and the impact of wrong treatments on the dynamics of the two diseases and their co-infection is determined. The disease-free equilibrium of the model is shown to be both locally and globally asymptotically stable when the basic reproduction number is less than one. Sensitivity analysis reveals that wrong treatments positively impact the spread of malaria and COVID-19 in the population, which agrees with the result from numerical simulation. Moreover, numerical simulation shows that those infected with malaria dominate the infection space. This can be naturally attributed to the endemicity of malaria in the population.

Keywords: endemic; co-infection; misdiagnosis; modeling

1. Introduction

Malaria is a mosquito-borne disease that spreads among humans through bites of infected female Anopheles mosquitoes. It has been reported that Malaria has caused millions of deaths among children and pregnant women alike in sub-Saharan Africa and other countries where the disease is endemic [1,2]. It is estimated that there are about 247 million cases of malaria globally, with over 619,000 malaria-related deaths. In these numbers, tropical regions in Africa accounted for 92% cases and 93% deaths, respectively, out of which Nigeria had the highest with 25% and Uganda the lowest with 4% [3,4]. Symptoms of malaria such as fever, headache, nausea, and muscular discomfort or weariness have been shown to mimic those of coronavirus disease (COVID-19), a disease believed to have emanated in Wuhan, China [5–7]. This overlap of symptoms of the two diseases has led to the loss of many lives due to misdiagnosis and wrong treatments, especially in countries where there is a shortage of sophisticated diagnostic equipment to clearly identify and differentiate between the two diseases [8,9].

Co-infection occurs when a host, whether human, animal, or plant, gets infected by two or more different germs (virus, bacteria, or parasite) at the same time or right after the other [10]. Co-infection can affect how sick the host becomes, make symptoms more difficult to read, or even make the host much sicker than a single germ would. Common co-infections include HIV and Tuberculosis, Flu and bacterial pneumonia, COVID-19 and flu, malaria and bacterial infection, Malaria and Zika virus, Ebola and malaria, Dengue and Zika virus, etc [11–13].

There have been documented cases of co-infection of malaria and COVID-19 in the areas where malaria is endemic [14–16]. Co-infection of malaria and COVID-19 occurs when a person is simultaneously infected with plasmodium that causes malaria and SARS-CoV-2 that causes COVID-19. This presents major health challenges with potential severe consequences. For example, Mohamed et al [17] presented a comprehensive and systematic review of clinical outcomes of co-infection of the two diseases. The review discovers that most patients who were co-infected with the two diseases experienced short-term hospitalization and mild to moderate disease severity. In Lopez et al [18], a population-based study about COVID-19 and malaria in Burkina Faso during the

first wave of the COVID-19 pandemic is presented. The study confirms a reasonable frequency of occurrence of co-infection of malaria and COVID-19 in African countries. In [19], there is a documentation of predominance of severe COVID-19 and a high proportion of adverse maternal-fetal outcomes among women who are co-infected with malaria and COVID-19. All these confirm the existence of co-infection of COVID-19 and malaria in the areas where the two diseases co-circulate. It is therefore obvious that the interaction between these two diseases can impose challenges in terms of diagnosis, treatment, and control. Hence, understanding the dynamics of the two diseases and their co-infection is important for developing effective control measures and optimizing health care strategies.

Mathematical models have been used over the past decades as a valuable tool for understanding the transmission dynamics of infectious diseases. Mathematical modeling of infectious diseases involves dividing the population under study into compartments based on the disease status, and using nonlinear differential equations to model the rates at which the compartments change at each time. Transmission dynamics of Individual diseases and their co-infections with one another have been modeled in this way, and important results have been obtained through rigorous model analyses and simulations. Since the outbreak of COVID-19 in 2019, many mathematical models have been proposed and used to understand the transmission dynamics of the disease. Some of the models can be found in [20–25] and the references therein. In Ojo and Goufo [26], the impact of COVID-19 on a malaria-endemic region is examined using a mathematical model. The major finding in this work is that COVID-19 cases will predominate in the populace and drives malaria to extinction when $\mathcal{R}_m < 1 < \mathcal{R}_c$, whereas malaria will drive COVID-19 to extinction when $\mathcal{R}_c < 1 < \mathcal{R}_m$ where $\mathcal{R}_c$ and $\mathcal{R}_m$ are the basic reproduction numbers for COVID-19 and malaria, respectively. The work further identifies that at endemic equilibrium, the two diseases will co-circulate, with the one with the higher reproduction number predominating but not eradicating the other. It is also shown that COVID-19 will invade a population where malaria is endemic if its invasion reproduction number is greater than unity. In Ren and Xue [27], co-infection of malaria and COVID-19 is modeled to understand the dynamics of the two diseases. The model is extended to optimal control using prevention and treatment as control measures for COVID-19 and malaria, respectively. The result of the optimal control analysis indicates that applying each control strategy alone has the capability of reducing the rate of co-circulation, but using prevention for COVID-19 increases the rate of malaria infection, and using prevention for malaria prolongs the period of COVID-19 infection.

To better capture the dynamics of COVID-19, many authors have extended the classical integer-order system of nonlinear differential equations to fractional-order systems, which have been proved to better capture memory effects and anomalous diffusion in disease transmission. Some notable fractional-order ordinary differential equation models for COVID-19 can be found in [28–30], and many others.

For a better understanding of the dynamics of malaria COVID-19 co-infection, we develop a mathematical model that incorporates the key aspects of both diseases, such as rates at which individuals get wrong treatment for either disease, endemicity of malaria in the population, etc. Simulation of the model will help to gain insight into the spread of the diseases, and also help to identify factors that contribute to the simultaneous spread of the diseases.

This research work is organized as follows: In Section 2, the model, with its analysis, is presented. The analysis performed on the model includes determination of the basic reproduction number of the disease, local and global asymptotic stability analyses of the disease-free equilibrium, and sensitivity analysis of the basic reproduction number. Simulation of the model is done in Section 3, and the work is summarized and concluded in Section 4.

2. Formulation of the Co-Infection Model

We consider a typical human and mosquito populations where malaria is endemic, and there is an outbreak of COVID-19. To model the dynamics of the two diseases and their possible co-infection, we divide the human and mosquito populations into eight (8) compartments and two (2) compartments, respectively. In human population, we have the susceptible class (S_h), the exposed class(E_h), those infected with malaria only (I_{hm}), those infected with COVID-19 only (I_{hc}), those co- infected with malaria and COVID-19 (I_{hmc}), those infected with malaria but wrongly treated for COVID-19(T_c), and those infected with COVID-19 but wrongly treated for malaria (T_m), and the recovered class (R_h). In the mosquito population, we have mosquitoes (S_v) that are susceptible to plasmodium infection, and mosquitoes (I_v) that are infected with the parasite. We assume that malaria infection starts in the human population when infected mosquitoes, I_v bite susceptible humans and infect them with malaria parasite. On the other hand, COVID-19 infection begins when the proportion $(\epsilon_1 + \epsilon_2)$ of the susceptible class becomes infected with coronavirus through successful contact with those in the compartments I_{hc}, I_{hmc} and T_m, with λ, as the contact rate. Due to the prevalence of malaria in the population under study, it is assumed that the exposed class, in general, is made up of 3 categories of persons: those already infected with malaria $(\epsilon_1 S_h)$, and are therefore exposed to COVID-19, those not infected with malaria already $(\epsilon_2 S_h)$, but are exposed to COVID-19 only, and those not infected with malaria, and are therefore exposed to malaria only, $(\epsilon_3 S_h)$. This subdivision of

the exposed class to reflect heterogeneous infection backgrounds follows a rationale analysis to compartmental structures in delayed epidemic models, where distinct exposed sub-populations reflect varying disease histories [31]. The compartments, I_{hm}, I_{hc} and I_{hmc} respectively comprises of the proportions $p_m E_h, p_c E_h$ and $p_{mc} E_h$, who are infected with malaria only, COVID-19 only, and both diseases, respectively. Co-infection of malaria and COVID-19 occurs when those infected with malaria become infected with COVID-19, and vice versa. We assume that those in the class I_{hm} may become co-infected with COVID-19 at the rate, α_{mc} to join the class, I_{hmc}, while those in the class I_{hc} joins the class after being co-infected with malaria at the rate α_{cm}. Additionally, individuals in the compartment, I_{hm} may be wrongly treated for COVID-19, at the rate τ_c' to join the class, T_c, while those in the class I_{hc}, may experience wrong treatment at the rate τ_m', to join the class, T_m. Individuals in the compartments, I_{hm} and T_c can recover from malaria at the rate, γ_m, with or without treatment, while I_{hc} and T_m can recover from COVID-19 at the rate γ_c. The class of co-infected individuals has a separate recovery rate given by γ_{mc}. Those that recover from the diseases, especially malaria, may become reinfected at the rate, δ. It is the assumption of the model that all the categories of humans experience the same natural death rate, σ_n, while the infected compartments suffer additional disease-related deaths at the appropriate rates. In the mosquito population, the susceptible mosquitoes become infected with malaria parasite when they successfully bite humans in the compartments I_{hm}, I_{hmc} and T_c. The mosquito biting rate is β, while the probabilities of transmission of the malaria parasite from humans to mosquito, and from mosquito to human are α_{hm} and α_{mh} respectively. The mosquitoes die naturally at the rate, σ_v. Table 1 shows the meaning and values of the parameters used in this model. These assumptions on the dynamics of the two diseases and their co-infection give rise to the flow diagram (Figure **??**) and the system of ordinary differential equations:

$$\begin{aligned}
\frac{dS_h(t)}{dt} &= \pi_h + \mu_h N_h + \delta R - \lambda(\epsilon_1+\epsilon_2)(I_{hc}+T_m+I_{hmc})\frac{S_h}{N_h} - \epsilon_3\alpha_{mh}\beta I_v\frac{S_h}{N_v} - \sigma_n S_h,\\
\frac{dE_h(t)}{dt} &= \lambda(\epsilon_1+\epsilon_2)(I_{hc}+T_m+I_{hmc})\frac{S_h}{N_h} + \epsilon_3\alpha_{mh}\beta I_v\frac{S_h}{N_v} - (p_m+p_{mc}+p_c+\sigma_n)E_h,\\
\frac{dI_{hm}(t)}{dt} &= p_m E - (\alpha_{mc}+\tau_c'+\gamma_m+\sigma_n+\sigma_m)I_{hm},\\
\frac{dI_{hc}(t)}{dt} &= p_c E - (\alpha_{cm}+\tau_m'+\gamma_c+\sigma_n+\sigma_c)I_{hc},\\
\frac{dI_{hmc}(t)}{dt} &= p_{mc}E + \alpha_{mc}I_{hm} + \alpha_{cm}I_{hc} - (\gamma_{mc}+\sigma_{mc}+\sigma_n)I_{hmc},\\
\frac{dT_c(t)}{dt} &= \tau_c' I_{hm} - (\gamma_m+\sigma_n+\sigma_m)T_c,\\
\frac{dT_m(t)}{dt} &= \tau_m' I_{hc} - (\gamma_c+\sigma_n+\sigma_c)T_m,\\
\frac{dR_h(t)}{dt} &= \gamma_m(T_c+I_{hm}) + \gamma_c(I_{hc}+T_m) + \gamma_{mc}I_{hmc} - (\delta+\sigma_n)R_h,\\
\frac{dS_v(t)}{dt} &= \pi_v + \mu_v N_v - \alpha_{hm}\beta(I_{hm}+T_c+I_{hmc})\frac{S_v}{N_h} - \sigma_v S_v,\\
\frac{dI_v(t)}{dt} &= \alpha_{hm}\beta(I_{hm}+T_c+I_{hmc})\frac{S_v}{N_h} - \sigma_v I_v,
\end{aligned} \tag{1}$$

with the initial conditions; $S_h(0) > 0, E_h(0) \geq 0, I_m(0) \geq 0, I_{hc}(0) \geq 0, I_{hmc}(0) \geq 0, T_c(0) \geq 0, T_m(0) \geq 0, R_h(0) \geq 0, S_v(0) > 0, I_v(0) \geq 0$. The total human population, N_h and total mosquito population N_v satisfy the following differential equations

$$\begin{aligned}
\frac{dN_h(t)}{dt} &= \pi_h + (\mu_h - \sigma_n)N_h - \sigma_m(I_{hm}+T_c) - \sigma_c(I_{hc}+T_m) - \sigma_{mc}I_{hmc},\\
\frac{dN_v(t)}{dt} &= \pi_v + (\mu_v - \sigma_v)N_v
\end{aligned}$$

with $N_h(0) > 0, N_v(0) > 0$. Therefore, the populations of humans and mosquitoes are not closed.

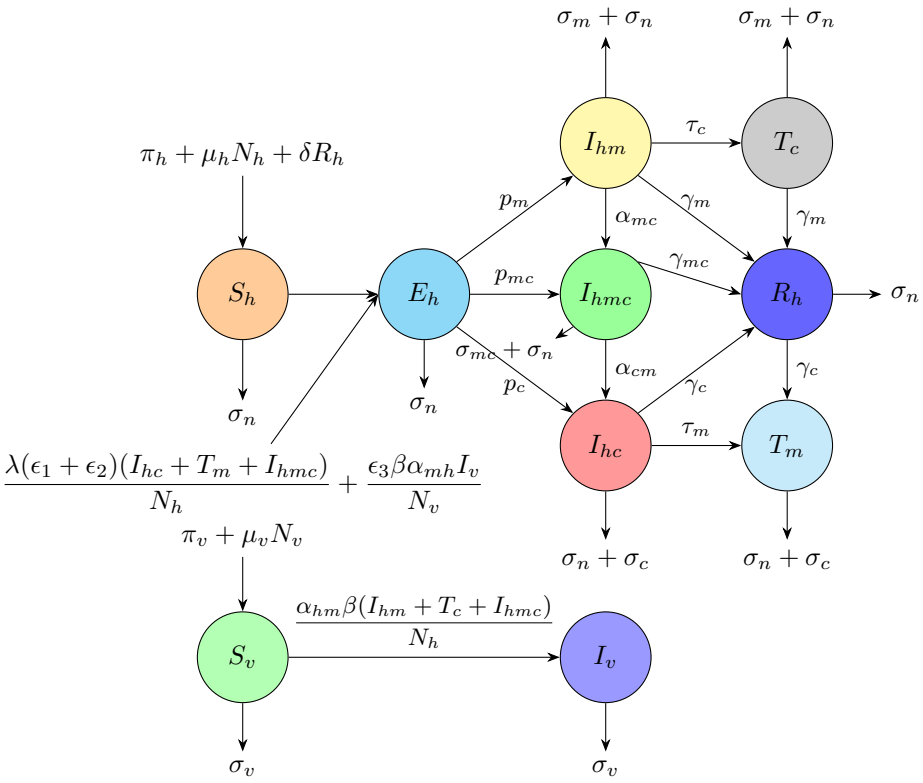

Figure 1. Flow diagram of compartment model

Table 1. Parameters used in the model.

Parameter	Meaning	Value	Source
ϵ_1	proportion of humans susceptible to COVID-19 only	0.2	assumed
ϵ_2	proportion of humans susceptible to malaria and COVID-19	0.5	assumed
ϵ_3	proportion of humans susceptible to malaria only	0.3	assumed
π_h	rate of recruitment of humans	1000	assumed
π_v	rate of recruitment of mosquitoes	1000	assumed
α_{hm}	probability of transmission of plasmodium from humans to mosquitoes	0.25	[32]
α_{mh}	probability of transmission of plasmodium from mosquitoes to humans	0.48	[32]
β	mosquito biting rate	0.56	assumed
σ_n	natural death of humans	0.00005	[33]
σ_m	malaria-induced death in humans	0.0019	[27]
σ_c	death due to COVID-19	0.015	[27]
σ_{mc}	death due to co-infection of the two diseases	0.5	assumed
λ	rate of contact between infectious and susceptible humans	0.4531	[34]
p_m	proportion of humans that are infected with malaria only	0.8333	[32]
p_{mc}	proportion of humans that are co-infected with malaria and COVID-19	0.25	assumed
p_c	proportion of humans that are infected with COVID-19 only	0.6	[35]
τ_m'	rate at which humans are wrongly treated for malaria	0.34	assumed
τ_c'	rate at which humans are wrongly treated for COVID-19	0.34	assumed
γ_m	rate of recovery from malaria	0.25	[33]
γ_c	rate of recovery from COVID-19	0.3	[36]
γ_{mc}	rate of recovery from co-infection	0.025	[37]
σ_v	natural death of mosquitoes	0.048	[33]
μ_h	rate of birth for humans	0.024	assumed
μ_v	rate of birth for mosquitoes	0.0126	assumed
δ	rate at which recovered humans become susceptible again	0.28	assumed
α_{mc}	proportion of malaria-infected humans that are co-infected with COVID-19	0.08333	[37]
α_{cm}	proportion of COVID-19-infected humans that are co-infected with malaria	0.4	[37]

2.1. Basic Reproduction Number

The disease-free equilibrium of the co-infection model is the steady state of the model system where there is no malaria, COVID-19, and their co-infection in the population. This is denoted by E_0^{mc}, and given by $E_0^{mc} = (S_h^*, 0, 0, 0, 0, 0, 0, 0, S_v^*, 0)$, where $S_h^* = \frac{\pi_h}{\sigma_n - \mu_h}, S_v^* = \frac{\pi_v}{\sigma_v - \mu_v}$, where $\sigma_n > \mu_h, \sigma_v > \mu_v$. With the disease-free equilibrium and application of the next-generation matrix(NGM) method, the basic reproduction number of co-infection of malaria and COVID-19 is

$$\mathcal{R}_{mc} = \frac{\mathcal{R}'_{0c} + \sqrt{\mathcal{R}'^2_{0c} + 4\mathcal{R}'_{0m}}}{2} \tag{2}$$

where

$$\mathcal{R}'_{0c} = \frac{\lambda(\epsilon_1 + \epsilon_2)(\alpha_{mc}p_m k_3 k_6 + \alpha_{cm}p_c k_2 k_6 + k_2 k_3 k_6 p_{mc} + k_2 k_4 k_6 p_c + k_2 k_4 p_c \tau'_m)}{k_1 k_3 k_4 k_6}$$

and

$$\mathcal{R}'_{0m} = \frac{\epsilon_3 \alpha_{mh}\alpha_{hm}\beta^2(\alpha_{mc}p_m k_3 k_5 + \alpha_{cm}p_c k_2 k_5 + k_2 k_4 k_5 p_{mc} + k_3 k_4 k_5 p_m + k_3 k_4 p_m \tau'_c)}{k_1 k_2 k_4 k_5 \sigma_v}$$

with $k_1 = p_m + p_{mc} + p_c + \sigma_n, k_2 = \tau'_c + \alpha_{mc} + \gamma_m + \sigma_n + \sigma_m, k_3 = \tau'_m + \alpha_{cm} + \gamma_c + \sigma_n + \sigma_c$, $k_4 = \gamma_{mc} + \sigma_n + \sigma_{mc}$, $k_5 = \gamma_m + \sigma_n + \sigma_m, k_6 = \gamma_c + \sigma_n + \sigma_c$. The expression (2) for the reproduction number is obtained as the spectral radius of the next generation matrix(NGM);

$$FV^{-1} = \begin{pmatrix} A_1 & \frac{\lambda(\epsilon_1+\epsilon_2)\alpha_{mc}}{k_2 k_4} & A_3 & \frac{\lambda(\epsilon_1+\epsilon_2)}{k_4} & 0 & \frac{\lambda(\epsilon_1+\epsilon_2)}{k_6} & \frac{\epsilon_3\alpha_{mh}S_h^*}{N_v^*\sigma_v} \\ 0 & 0 & 0 & 0 & 0 & 0 & 0 \\ 0 & 0 & 0 & 0 & 0 & 0 & 0 \\ 0 & 0 & 0 & 0 & 0 & 0 & 0 \\ 0 & 0 & 0 & 0 & 0 & 0 & 0 \\ 0 & 0 & 0 & 0 & 0 & 0 & 0 \\ A_2 & A_4 & \frac{\alpha_{hm}\alpha_{cm}S_v^*}{N_h^* k_3 k_4} & \frac{\alpha_{hm}S_v^*}{N_h^* k_4} & \frac{\alpha_{hm}S_v^*}{N_h^* k_5} & 0 & 0 \end{pmatrix} \tag{3}$$

where

$$A_1 = \frac{\lambda(\epsilon_1 + \epsilon_2)}{k_1}\left[\frac{p_c}{k_3} + \frac{p_{mc}}{k_4} + \frac{p_c\tau'_m}{k_3 k_6} + \frac{\alpha_{mc}p_m}{k_2 k_4} + \frac{\alpha_{cm}p_c}{k_3 k_4}\right],$$

$$A_2 = \frac{\alpha_{hm}S_v^*}{N_h^* k_1}\left[\frac{p_m}{k_2} + \frac{p_{mc}}{k_4} + \frac{p_m\tau'_c}{k_2 k_5} + \frac{\alpha_{mc}p_m}{k_2 k_4} + \frac{\alpha_{cm}p_c}{k_3 k_4}\right],$$

$$A_3 = \frac{\lambda(\epsilon_1 + \epsilon_2)}{k_3}\left[1 + \frac{\alpha_{cm}}{k_4} + \frac{\tau'_m}{k_6}\right],$$

$$A_4 = \frac{\alpha_{hm}S_v^*}{N_h^* k_2}\left[1 + \frac{\alpha_{mc}}{k_4} + \frac{\tau'_c}{k_5}\right].$$

The matrices F and V are given by

$$F = \begin{pmatrix} 0 & 0 & \lambda(\epsilon_1 + \epsilon_2) & \lambda(\epsilon_1 + \epsilon_2) & 0 & \lambda(\epsilon_1 + \epsilon_2) & \epsilon_3\alpha_{mh}\beta\frac{S_h^*}{N_v^*} \\ 0 & 0 & 0 & 0 & 0 & 0 & 0 \\ 0 & 0 & 0 & 0 & 0 & 0 & 0 \\ 0 & 0 & 0 & 0 & 0 & 0 & 0 \\ 0 & 0 & 0 & 0 & 0 & 0 & 0 \\ 0 & 0 & 0 & 0 & 0 & 0 & 0 \\ 0 & \alpha_{hm}\beta\frac{S_v^*}{N_h^*} & 0 & \alpha_{hm}\beta\frac{S_v^*}{N_h^*} & \alpha_{hm}\beta\frac{S_v^*}{N_h^*} & 0 & 0 \end{pmatrix}$$

and $V = \begin{pmatrix} k_1 & 0 & 0 & 0 & 0 & 0 & 0 \\ -p_m & k_2 & 0 & 0 & 0 & 0 & 0 \\ -p_c & 0 & k_3 & 0 & 0 & 0 & 0 \\ -p_{mc} & -\alpha_{mc} & -\alpha_{cm} & k_4 & 0 & 0 & 0 \\ 0 & -\tau_c' & 0 & 0 & k_5 & 0 & 0 \\ 0 & 0 & -\tau_m & 0 & 0 & k_6 & 0 \\ 0 & 0 & 0 & 0 & 0 & 0 & \sigma_v \end{pmatrix}$, respectively.

The next generation matrix (3) has two nonzero eigenvalues namely, $\frac{\mathcal{R}_{0c}'+\sqrt{\mathcal{R}_{0c}'^2+4\mathcal{R}_{0m}'}}{2}$ and $\frac{\mathcal{R}_{0c}'-\sqrt{\mathcal{R}_{0c}'^2+4\mathcal{R}_{0m}'}}{2}$, It is obvious that $\frac{\mathcal{R}_{0c}'+\sqrt{\mathcal{R}_{0c}'^2+4\mathcal{R}_{0m}'}}{2} > \frac{\mathcal{R}_{0c}'-\sqrt{\mathcal{R}_{0c}'^2+4\mathcal{R}_{0m}'}}{2}$ since $\mathcal{R}_{0c}' < \sqrt{\mathcal{R}_{0c}'^2+4\mathcal{R}_{0m}'}$. Hence, (2) is obtained.

- The basic reproduction number (2) gives explicitly, the average number of persons that can be infected with malaria, COVID-19 or both, by one index case of malaria and one index case of COVID-19, in their infectious lifetimes when introduced in a purely susceptible population. This form of the basic reproduction number is different from what is found in the literature, where the reproduction number of co-infection of two diseases is obtained as the maximum of the reproduction numbers of the individual diseases [38–40].
- Note that $\mathcal{R}_{0c}'$ can be written in terms of $\mathcal{R}_{0c}$ as

$$\mathcal{R}_{0c}' = (\epsilon_1+\epsilon_2)\frac{k_1^{covid}}{k_1}\frac{k_3'}{k_3}\mathcal{R}_{0c} + \frac{(\epsilon_1+\epsilon_2)\lambda}{k_1}\left(\frac{p_{mc}}{k_4}+\frac{p_c\tau_m'}{k_3k_6}+\frac{\alpha_{mc}p_m}{k_2k_4}+\frac{\alpha_{cm}p_c}{k_3k_4}\right)$$

where $k_1^{covid} = p_c+\sigma_n$, $k_3' = \gamma_c+\sigma_n+\sigma_c$. Here, $\mathcal{R}_{0c} = \frac{\lambda p_c}{(p_c+\sigma_n)(\gamma_c+\sigma_n+\sigma_c)}$ is the basic reproduction number of COVID-19. and $\mathcal{R}_{0m}'$ can be written in terms of $\mathcal{R}_{0m}$

$$\mathcal{R}_{0m}' = \epsilon_3\frac{k_1^{malaria}}{k_1}\frac{k_2'}{k_2}\mathcal{R}_{0m}^2 + \frac{\epsilon_3\alpha_{mh}\alpha_{hm}\beta^2}{k_1\sigma_v}\left(\frac{p_{mc}}{k_4}+\frac{p_m\tau_c'}{k_2k_5}+\frac{\alpha_{mc}p_m}{k_2k_4}+\frac{\alpha_{cm}p_c}{k_3k_4}\right)$$

where $k_1^{malaria} = p_m+\sigma_n$, $k_2' = \gamma_m+\sigma_m+\sigma_n$. Here, $\mathcal{R}_{0m} = \left(\frac{\alpha_{mh}\alpha_{hm}\beta^2 p_m}{\sigma_v(p_m+\sigma_n)(\gamma_m+\sigma_m+\sigma_n)}\right)^{\frac{1}{2}}$ is the basic reproduction number of malaria.
- In $\mathcal{R}_{mc}$, if there is no malaria, i.e $\mathcal{R}_{0m}' = 0$, then $\mathcal{R}_{mc} = \frac{\mathcal{R}_{0c}'}{2}+\frac{\mathcal{R}_{0c}'}{2} = \mathcal{R}_{0c}'$. Furthermore, in the absence of malaria, $\epsilon_1 = 0, \epsilon_2 = 1, p_m = p_{mc} = \tau_m' = \alpha_{cm} = \alpha_{mc} = 0$. Also, $p_m = p_{mc} = 0 \Rightarrow k_1 = k_1^{covid}$, and $\tau_m' = 0 \Rightarrow k_3 = k_3'$. In this case, $\mathcal{R}_{mc}$ reduces to $\mathcal{R}_{0c}$, the basic reproduction number of COVID-19.
On the other hand, if there is no COVID-19 infection in the population, then $\mathcal{R}_{0c}' = 0$, and $\mathcal{R}_{mc} = \sqrt{\mathcal{R}_{0m}'}$. Furthermore, $\epsilon_3 = 1, p_{mc} = p_c = \tau_c' = \alpha_{cm} = \alpha_{mc} = 0$. Also, $p_m = p_{mc} = 0 \Rightarrow k_1 = k_1^{malaria}$, and $\tau_c' = 0 \Rightarrow k_2 = k_2'$. In this case, $\mathcal{R}_{mc}$ reduces to the basic reproduction number of malaria, $\mathcal{R}_{0m}$.

2.2. Local Stability of the Disease-Free Equilibrium

In the Jacobian matrix of the model system, we delete the rows and columns that correspond to non-diseased classes, S_h, R and S_v, since their diagonal entries are the only entries in their respective columns and are all negative. Hence, we work with the submatrix

$$J(E_0^{mc}) = \begin{pmatrix} -k_1 & 0 & \lambda(\epsilon_1+\epsilon_2) & \lambda(\epsilon_1+\epsilon_2) & 0 & \lambda(\epsilon_1+\epsilon_2) & \epsilon_3\alpha_{mh}\beta\frac{S_h^*}{N_v^*} \\ p_m & -k_2 & 0 & 0 & 0 & 0 & 0 \\ p_{mc} & 0 & -k_3 & 0 & 0 & 0 & 0 \\ p_c & \alpha_{mc} & \alpha_{cm} & -k_4 & 0 & 0 & 0 \\ 0 & \tau_c' & 0 & 0 & -k_5 & 0 & 0 \\ 0 & 0 & \tau_m' & 0 & 0 & -k_6 & 0 \\ 0 & \alpha_{hm}\beta\frac{S_v^*}{N_h^*} & 0 & \alpha_{hm}\beta\frac{S_v^*}{N_h^*} & \alpha_{hm}\beta\frac{S_v^*}{N_h^*} & 0 & -\sigma_v \end{pmatrix},$$

Observe that $J(E_0^{mc}) = F - V$, where F and V are as obtained in Subsection 4.1. Hence, by Theorem 2 in [41], all the eigenvalues of $J(E_0^{mc})$ have negative real part if $\mathcal{R}_{mc} := \rho(FV^{-1}) < 1$. This shows local asymptotic stability of E_0^{mc} if $\mathcal{R}_{mc} < 1$. This implies that malaria, COVID-19, and their co-infection can be controlled if the initial number of infected humans and mosquitoes are in the basin of attraction of the disease-free equilibrium.

2.3. Global Stability of Disease-Free Equilibrium

Consider the system

$$\begin{aligned}\frac{dS_h(t)}{dt} &= \pi_h + (\mu_h - \sigma_n)S_h + \delta R,\\ \frac{dR_h(t)}{dt} &= -(\sigma_n + \delta)R_h(t),\\ \frac{dS_v(t)}{dt} &= \pi_v + (\mu_v - \sigma_v)S_v,\end{aligned} \tag{4}$$

involving only the uninfected population, and the system

$$\begin{aligned}\frac{dE_h(t)}{dt} &= \lambda(\epsilon_1+\epsilon_2)\frac{(I_{hc}+T_m+I_{hmc})}{N_h}S_h + \frac{\epsilon_3\alpha_{mh}\beta I_v S_h}{N_v} - (p_m+p_{mc}+p_c+\sigma_n)E_h,\\ \frac{dI_{hm}(t)}{dt} &= p_m E - (\alpha_{mc}+\tau_c'+\gamma_m+\sigma_n+\sigma_m)I_{hm},\\ \frac{dI_{hc}(t)}{dt} &= p_c E - (\alpha_{cm}+\gamma_c+\tau_m'+\sigma_n+\sigma_c)I_{hc},\\ \frac{dI_{hmc}(t)}{dt} &= p_{mc}E + \alpha_{mc}I_{hm} + \alpha_{cm}I_{hc} - (\gamma_{mc}+\sigma_n+\sigma_{mc})I_{hmc},\\ \frac{dT_c(t)}{dt} &= \tau_c' I_{hm} - (\gamma_m+\sigma_n+\sigma_m)T_c(t),\\ \frac{dT_m(t)}{dt} &= \tau_m' I_{hc} - (\gamma_c+\sigma_n+\sigma_c)T_m(t),\\ \frac{dI_v(t)}{dt} &= \frac{\alpha_{hm}\beta(I_{hm}+T_c+I_{hmc})}{N_h}S_v - \sigma_v I_v,\end{aligned} \tag{5}$$

involving only the infected populations. The solution to (4) is easily obtained as

$$\begin{aligned}S_h(t) &= S_h^* - (S_h^* - S(0) - R_h(0))\,e^{-(\sigma_n-\mu_h)t} - R(0)e^{-(\delta+\sigma_n)t}\\ R_h(t) &= R_h(0)e^{-(\delta+\sigma_n)t}\\ S_v(t) &= S_v^* - (S_v^* - S_v(0))\,e^{-(\sigma_v-\mu_v)t}\end{aligned} \tag{6}$$

From the subsystem (5), we have that

$$J(E^{mc}) - \Phi(E_h, I_{hm}, I_{hc}, I_{hmc}, T_c, T_m, I_v) = \begin{pmatrix} \epsilon_3\alpha_{mh}\beta I_v\left(\frac{S_h^*}{N_v^*} - \frac{S_h}{N_v}\right) + \lambda(\epsilon_1+\epsilon_2)(I_{hc}+T_m+I_{hmc})\left(\frac{S_h^*}{N_h^*} - \frac{S_h}{N_h}\right)\\ 0\\ 0\\ 0\\ 0\\ 0\\ \alpha_{hm}\beta(I_{hm}+T_c+I_{hmc})\left(\frac{S_v^*}{N_h^*} - \frac{S_v}{N_h}\right)\end{pmatrix} \tag{7}$$

where $\Phi(E_h, I_{hm}, I_{hc}, I_{hmc}, T_c, T_m, I_v)$ is the right-hand side of (5). It is easy to see that (7) is nonnegative since from (6), $S_h(t) \le S_h^*, N_h(t) \le N_h^*, N_v(t) \le N_v^*$ and $S_v(t) \le S_v^*$, where $S_h^* = N_h^* = \frac{\pi_h}{\sigma_n-\mu_h}$ and $S_v^* = N_v^* = \frac{\pi_v}{\sigma_v-\mu_v}$. More so, we note that as $t \to \infty$, the solution to (4) tends to the disease-free equilibrium, $\left(\frac{\pi_h}{\sigma_n-\mu_h}, 0, \frac{\pi_v}{\sigma_v-\mu_v}\right)$ of the subsystem because $e^{-(\sigma_n-\mu_h)t} \to 0$, $e^{-(\sigma_v-\mu_v)t} \to 0$ as $t \to \infty$. Hence, by theorem in Section 3 of [42], the disease-free equilibrium of the co-infection model is globally asymptotically stable. This shows that malaria, COVID-19, and their co-infection can be eradicated with appropriate control measures irrespective of the initial population of infected humans and mosquitoes.

2.4. Sensitivity Analysis of $\mathcal{R}_{mc}$

To investigate the impact of rate of wrong treatments and other parameters on the dynamics of the diseases, we perform a sensitivity analysis of $\mathcal{R}_{mc}$ with respect to τ_c' and τ_m', and other parameters in the basic reproduction number. The normalized forward sensitivity index of the reproduction, $\mathcal{R}_{mc}$ that depends on the parameter say, x is given by $\mathcal{S}_x^{\mathcal{R}_{mc}} = \frac{\partial\mathcal{R}_{mc}}{\partial x} \times \frac{x}{\mathcal{R}_{mc}}$. Using chain rule, and the fact that $\sqrt{\mathcal{R}_{0c}'^2 + 4\mathcal{R}_{0m}'} = 2\mathcal{R}_{mc} - \mathcal{R}_{0c}'$, we have that

$$\mathcal{S}_{\tau_c'}^{\mathcal{R}_{mc}} = \frac{\partial\mathcal{R}_{mc}}{\partial\tau_c'} \times \frac{\tau_c'}{\mathcal{R}_{mc}} = \frac{\partial\mathcal{R}_{mc}}{\partial\mathcal{R}_{0m}'} \times \frac{\partial\mathcal{R}_{0m}'}{\partial\tau_c'} \times \frac{\tau_c'}{\mathcal{R}_{mc}} = \frac{\epsilon_3\alpha_{mh}\alpha_{hm}\beta^2 p_m\tau_c' k_3k_5p_m(k_1k_3k_4^2k_2' - k_4 - \alpha_{mc})}{k_1^2k_2^2k_3^2k_4^2k_5^2\sigma_v^2\sqrt{\mathcal{R}_{0c}'^2 + 4\mathcal{R}_{0m}'}\mathcal{R}_{mc}}$$

$$= \frac{\epsilon_3\alpha_{mh}\alpha_{hm}\beta^2 p_m\tau_c' k_5p_m(k_1k_4^2k_2' - k_4 - \alpha_{mc})}{k_1^2k_2^2k_4^2k_5^2\sigma_v^2(2\mathcal{R}_{mc} - \mathcal{R}_{0c}')\mathcal{R}_{mc}},$$

$$\mathcal{S}_{\tau'_m}^{\mathcal{R}_{mc}} = \frac{\partial \mathcal{R}_{mc}}{\partial \tau'_m} \times \frac{\tau'_m}{\mathcal{R}_{mc}} = \frac{\partial \mathcal{R}_{mc}}{\partial \mathcal{R}'_{0c}} \times \frac{\partial \mathcal{R}'_{0c}}{\partial \tau'_m} \times \frac{\tau'_m}{\mathcal{R}_{mc}}$$

$$= \frac{1}{2}\left(1 + \frac{\mathcal{R}'_{0c}}{\sqrt{\mathcal{R}'^2_{0c} + 4\mathcal{R}'_{0m}}}\right) \frac{(\epsilon_1+\epsilon_2)\lambda p_c \tau'_m k_2 k_6 p_c (k_1 k_4^2 k'_3 - k_4 - \alpha_{cm})}{k_1^2 k_3^2 k_4^2 k_6^2 \mathcal{R}_{mc}}$$

$$= \frac{(\epsilon_1+\epsilon_2)\lambda p_c \tau'_m k_2 k_6 p_c (k_1 k_4^2 k'_3 - k_4 - \alpha_{cm})}{k_1^2 k_3^2 k_4^2 k_6^2 (2\mathcal{R}_{mc} - \mathcal{R}'_{0c})}$$

$$\mathcal{S}_{\alpha_{mh}}^{\mathcal{R}_{mc}} = \frac{\partial \mathcal{R}_{mc}}{\partial \alpha_{mh}} \times \frac{\alpha_{mh}}{\mathcal{R}_{mc}} = \frac{1}{2} \times \frac{4}{2} \times \frac{1}{\sqrt{\mathcal{R}'^2_{0c} + 4\mathcal{R}'_{0m}}} \times \frac{\mathcal{R}'_{0m}}{\alpha_{mh}} \times \frac{\alpha_{mh}}{\mathcal{R}_{mc}} = \frac{\mathcal{R}'_{0m}}{\mathcal{R}_{mc}\sqrt{\mathcal{R}'^2_{0c} + 4\mathcal{R}'_{0m}}} = \mathcal{S}_{\alpha_{hm}}^{\mathcal{R}_{mc}} = \mathcal{S}_{\epsilon_3}^{\mathcal{R}_{mc}}$$

$$\mathcal{S}_{\alpha_{hm}}^{\mathcal{R}_{mc}} = \frac{\partial \mathcal{R}_{mc}}{\partial \alpha_{hm}} \times \frac{\alpha_{hm}}{\mathcal{R}_{mc}} = \frac{1}{2} \times \frac{4}{2} \times \frac{1}{\sqrt{\mathcal{R}'^2_{0c} + 4\mathcal{R}'_{0m}}} \times \frac{\mathcal{R}'_{0m}}{\alpha_{hm}} \times \frac{\alpha_{hm}}{\mathcal{R}_{mc}} = \frac{\mathcal{R}'_{0m}}{\mathcal{R}_{mc}\sqrt{\mathcal{R}'^2_{0c} + 4\mathcal{R}'_{0m}}}$$

$$\mathcal{S}_{\beta}^{\mathcal{R}_{mc}} = \frac{\partial \mathcal{R}_{mc}}{\partial \beta} \times \frac{\beta}{\mathcal{R}_{mc}} = \frac{1}{2} \times \frac{4}{2} \times \frac{2\beta}{\sqrt{\mathcal{R}'^2_{0c} + 4\mathcal{R}'_{0m}}} \times \frac{\mathcal{R}'_{0m}}{\beta} \times \frac{\beta}{\mathcal{R}_{mc}} = \frac{2\mathcal{R}'_{0m}}{\mathcal{R}_{mc}\sqrt{\mathcal{R}'^2_{0c} + 4\mathcal{R}'_{0m}}}$$

$$\mathcal{S}_{\epsilon_1}^{\mathcal{R}_{mc}} = \frac{\partial \mathcal{R}_{mc}}{\partial \epsilon_1} \times \frac{\epsilon_1}{\mathcal{R}_{mc}} = \frac{\partial \mathcal{R}_{mc}}{\partial \mathcal{R}'_{0c}} \times \frac{\partial \mathcal{R}'_{0c}}{\partial \epsilon_1} \times \frac{\epsilon_1}{\mathcal{R}_{mc}} = \frac{1}{2}\left(1 + \frac{\mathcal{R}'_{0c}}{\sqrt{\mathcal{R}'^2_{0c} + 4\mathcal{R}'_{0m}}}\right) \times \frac{\mathcal{R}'_{0c}}{\epsilon_1+\epsilon_2} \times \frac{\epsilon_1}{\mathcal{R}_{mc}}$$

$$= \frac{1}{2}\left(\frac{2\mathcal{R}_{mc} - \mathcal{R}'_{0c} + \mathcal{R}'_{0c}}{2\mathcal{R}_{mc} - \mathcal{R}'_{0c}}\right) \times \frac{\mathcal{R}'_{0c}}{\epsilon_1+\epsilon_2} \times \frac{\epsilon_1}{\mathcal{R}_{mc}} = \frac{\mathcal{R}'_{0c}}{2\mathcal{R}_{mc} - \mathcal{R}'_{0c}} \frac{\epsilon_1}{\epsilon_1+\epsilon_2} = \mathcal{S}_{\epsilon_2}^{\mathcal{R}_{mc}}$$

$$\mathcal{S}_{\lambda}^{\mathcal{R}_{mc}} = \frac{\partial \mathcal{R}_{mc}}{\partial \lambda} \times \frac{\lambda}{\mathcal{R}_{mc}} = \frac{\partial \mathcal{R}_{mc}}{\partial \mathcal{R}'_{0c}} \times \frac{\partial \mathcal{R}'_{0c}}{\partial \lambda} \times \frac{\lambda}{\mathcal{R}_{mc}} = \frac{1}{2}\left(1 + \frac{\mathcal{R}'_{0c}}{\sqrt{\mathcal{R}'^2_{0c} + 4\mathcal{R}'_{0m}}}\right) \times \frac{\mathcal{R}'_{0c}}{\lambda} \times \frac{\lambda}{\mathcal{R}_{mc}}$$

$$= \frac{1}{2}\left(\frac{2\mathcal{R}_{mc} - \mathcal{R}'_{0c} + \mathcal{R}'_{0c}}{2\mathcal{R}_{mc} - \mathcal{R}'_{0c}}\right) = \frac{\mathcal{R}'_{0c}}{2\mathcal{R}_{mc} - \mathcal{R}'_{0c}}$$

$$\mathcal{S}_{\sigma_v}^{\mathcal{R}_{mc}} = \frac{\partial \mathcal{R}_{mc}}{\partial \sigma_v} \times \frac{\sigma_v}{\mathcal{R}_{mc}} = \frac{\partial \mathcal{R}_{mc}}{\partial \mathcal{R}'_{0m}} \times \frac{\partial \mathcal{R}'_{0m}}{\partial \sigma_v} \times \frac{\sigma_v}{\mathcal{R}_{mc}} = -\frac{\mathcal{R}'_{0m}}{k_1 k_2 k_4 k_5 \sigma_v \sqrt{\mathcal{R}'^2_{0c} + 4\mathcal{R}'_{0m}}} \times \frac{\sigma_v}{\mathcal{R}_{mc}}$$

$$= -\frac{\mathcal{R}'_{0m}}{k_1 k_2 k_4 k_5 \mathcal{R}_{mc}(2\mathcal{R}_{mc} - \mathcal{R}'_{0c})}$$

In Table 2, we have the numerical values of the sensitivity indices of these and other model parameters in the basic reproduction number. From the table, the most sensitive parameter is λ; the rate of contact between those infected with COVID-19 and the susceptible class. This indicates the need to reduce the contact rate in order to reduce the spread of COVID-19. Other important parameters are the mosquito biting rate (β), the probabilities of transmission of the malaria parasite from mosquito to human, and vice versa, and the rates of co-infections (α_{mc}, α_{cm}). The values of the parameters with positive sensitivity index should be reduced in order to manage the spread of malaria and COVID-19. The sensitivity index for death rate (σ_v) of mosquitoes, indicates the need to increase the rate at which mosquitoes are eliminated. Hence, more efforts should be centered on killing adult mosquitoes, and more importantly, on destroying those at their early stages of development.

Table 2. Sensitivity indices of some parameters in the basic reproduction number.

Parameter	Index	Parameter	Index
λ	0.9	β	0.55
α_{mh}	0.03	α_{hm}	0.03
p_m	0.08	p_c	0.02
p_{mc}	0.012	ϵ_1	0.03
ϵ_2	0.007	ϵ_3	0.032
α_{mc}	0.15	α_{cm}	0.0158
σ_v	-0.004	τ'_c	0.025
τ'_m	0.14		

3. Numerical Simulation and Discussion

In this section, the model is simulated using the parameter values in Table 1. The simulation tracks the dynamics of infectious populations under three different epidemiological scenarios: Malaria-only, COVID-19-only,

and their co-infection in a malaria-endemic population. Each scenario provides insights into how these diseases interact in a malaria-endemic setting and their respective impacts over time. The results of the numerical experiments are presented in Figures 2 and 3, to display the long-term behavior of malaria and COVID-19 in malaria-endemic population. The graphs show that in a malaria-endemic population, the number of persons infected with malaria only is the highest compared to those infected with COVID-19 or both. This is followed by those that are co-infected by the two diseases. Figure 4 displays the dynamics of those that are wrongly treated for malaria (T_c) and those that are wrongly treated for COVID-19 (T_m). The graphs show that the number of persons who have malaria but are treated for COVID-19 is higher than the number of those who are infected with COVID-19 but are treated for malaria. This agrees with Figures 2 and 3, where it is shown that the number of persons that are infected with malaria outnumbers those that are infected with COVID-19. Figure 5 shows the effect of the rates (τ_c') and (τ_m') of applying wrong treatments to the I_{hm} and I_{hc}, respectively. The graphs confirm that an increase in the rate, (τ_c'), of wrong treatment increases the number of those who are infected with malaria. Similarly, as the rate, (τ_m'), of wrong treatment increases, the number of persons that are infected with COVID-19 as increases. In the case of malaria, as wrong treatments are applied to I_{hm}, they remain infectious with malaria, and still infect susceptible mosquitoes, which become infectious and infect susceptible humans. This increases the number of persons in the compartment, I_{hm}. Similarly, in the case of COVID-19, as wrong treatments are applied to I_{hc}, they remain infectious, and infect humans that are susceptible to COVID-19 in the population. Thereby, increasing the number of those who are infected with COVID-19.

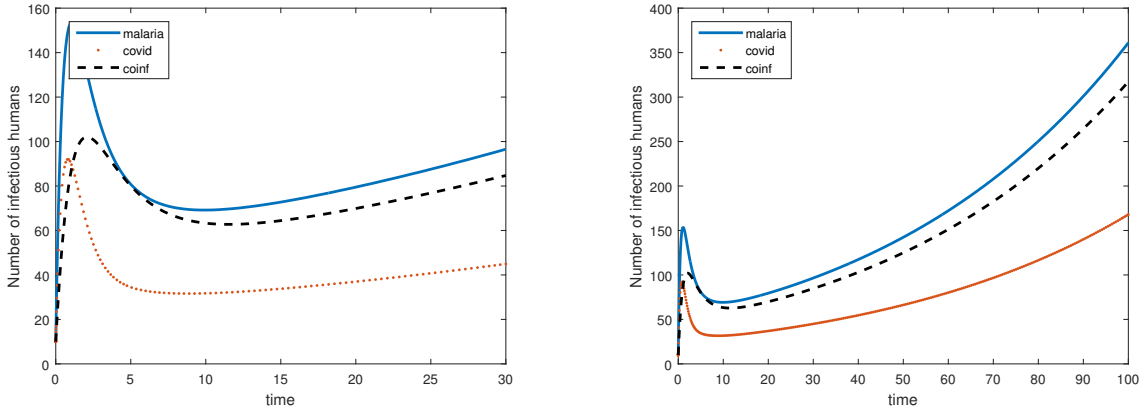

Figure 2. (**a**) Graph showing I_{hm}, I_{hc} and I_{hmc} for T = 30; (**b**) Graph showing I_{hm}, I_{hc} and I_{hmc} for T = 100.

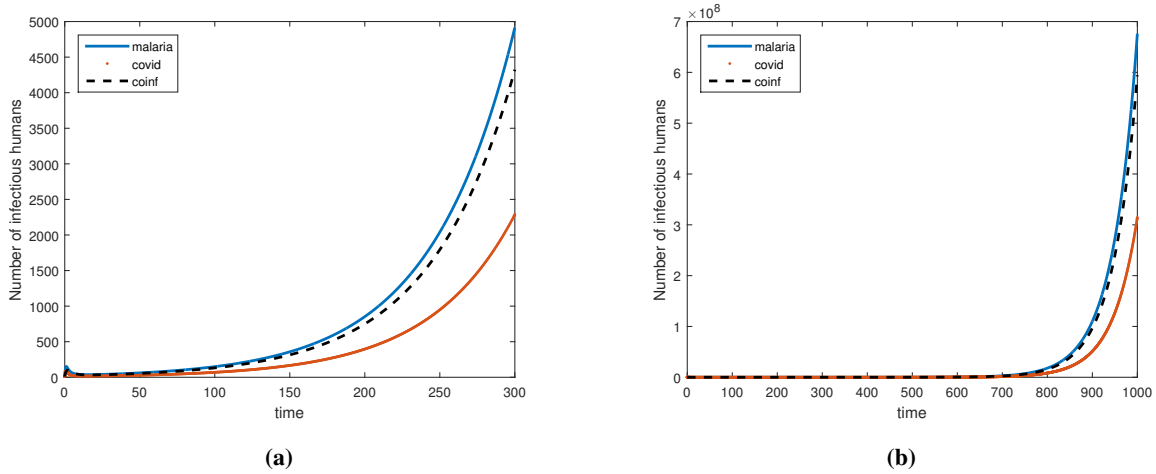

Figure 3. (**a**) Graph showing I_{hm}, I_{hc} and I_{hmc} for T = 300; (**b**) Graph showing I_{hm}, I_{hc} and I_{hmc} for T = 1000.

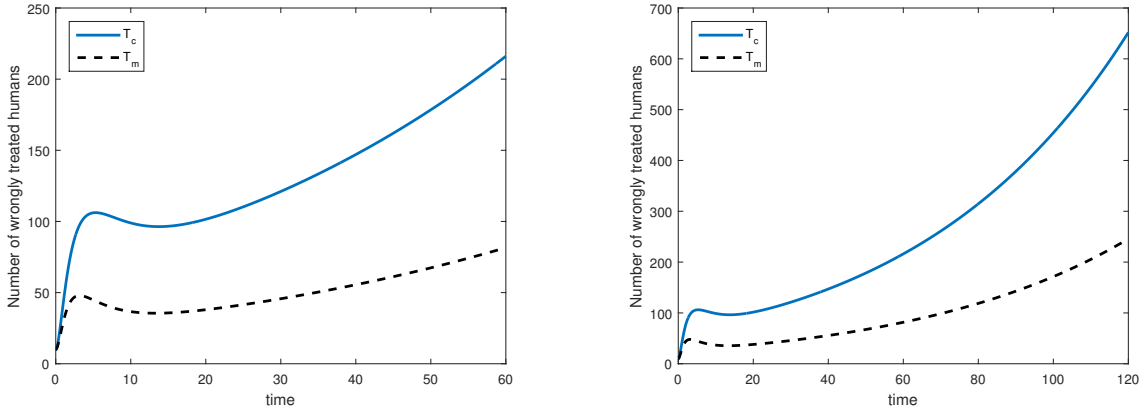

Figure 4. (**a**) Graph showing T_c and T_m for T = 60; (**b**) Graph showing T_c and T_m for T = 120.

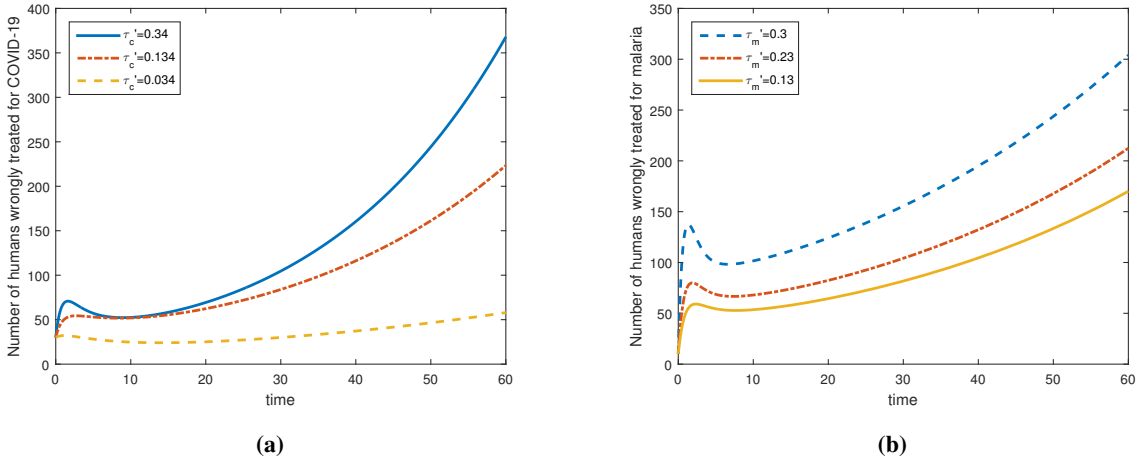

Figure 5. (**a**) Effect of wrong treatment rate (τ_c') on I_{hm}; (**b**) Effect of wrong treatment rate (τ_m') on I_{hc}

4. Summary and Conclusions

In this paper, a system of nonlinear ordinary differential equations is used to model the transmission dynamics of malaria, COVID-19, and their co-infection in the human population where malaria is endemic. The basic reproduction is obtained, which gives the average number of persons that can be infected with malaria, COVID-19, or both, by one infectious mosquito and an index case of COVID-19, in their entire infectious lifetime when introduced in a disease-free human and mosquito population. The disease-free equilibrium is both locally and globally asymptotically stable when the basic reproduction number is less than one. This points to the possibility of eradicating the disease, irrespective of the initial sizes of the infected population, if appropriate control measures are applied. Sensitivity indices of the parameters in the basic reproduction number reveal that reducing the rate of contact between susceptible and infected humans can help reduce the spread of COVID-19. Furthermore, the negativity of the sensitivity index of mosquito death rate confirms mosquito eradication as an effective control for stopping the menace of malaria. Numerical simulations ultimately reveal the endemicity of malaria in the population under study by showing the dominance of those infected with malaria, followed by those co-infected with malaria and COVID-19. This further shows that in a population where two or more infectious diseases co-circulate, those that are co-infected with the diseases cannot be more than those that are infected with the individual diseases.

In conclusion, this research contributes to the broader understanding of malaria and COVID-19 co-infection dynamics. Future research directions could be to integrate real-world data to improve the accuracy and predictive capabilities of co-infection models, thereby giving the opportunity for the development of targeted health care and health intervention strategies for effective management of the diseases. Based on the outcome of the sensitivity analysis, it is possible to extend the model in this paper by including the various control measures necessary for combating malaria and COVID-19. Optimal control and cost-effective analyses can be performed to optimally apply the different control measures for effective management of the diseases.

Author Contributions

M.C.A.: conceptualization, methodology, writing—original draft preparation; E.C.D.: software, writing—reviewing and editing, visualization. All authors have read and agreed to the published version of the manuscript.

Funding

This research received no external funding.

Institutional Review Board Statement

Not applicable.

Informed Consent Statement

Not applicable.

Data Availability Statement

Not applicable.

Conflicts of Interest

The authors declare no conflict of interest.

Use of AI and AI-Assisted Technologies

No AI tools were utilized for this paper.

References

1. Diabaté, A.B.; Sangaré, B.; Koutou, O. Optimal Control Analysis of a Mathematical Model of Malaria and COVID-19 Co-Infection Dynamics. *J. Biol. Dyn.* **2025**, *19*, 2568392. https://doi.org/10.1080/17513758.2025.2568392.
2. World Health Organization Malaria. Available online: https://www.who.int/news-room/fact-sheets/detail/malaria (accessed on 4 March 2025).
3. Duru, E.C.; Anyanwu, M.C.; Mbah, G.C.E. A Mathematical Model to Investigate the Effect of Misdiagnosis and Wrong Treatment in the Co-Circulation and Co-Infection of Malaria and Zika Virus Disease. *Bull. Biomath.* **2025**, *3*, 79–110. https://doi.org/10.59292/bulletinbiomath.1711811.
4. Nancy, A.M.; Shichika, J.M.; Bii, A. Mathematical Modelling of Malaria Transmission Dynamics in Kenya: The Role of Seasonality, Drug Resistance, and Human Movement. *Asian J. Adv. Res. Rep.* **2025**, *19*, 456–468. https://doi.org/10.9734/ajarr/2025/v19i71111.
5. Asamoah, I.; Adusei-Poku, M.; Vandyck-Sey, P.; et al. COVID-19 in Patients Presenting with Malaria-like Symptoms at a Primary Healthcare Facility in Accra, Ghana. *PLOS ONE* **2024**, *19*, e0298088. https://doi.org/10.1371/journal.pone.0298088.
6. Prabhu, S.R.; Ware, A.P.; Saadi, A.V.; et al. Malaria Epidemiology and COVID-19 Pandemic: Are They Interrelated? *OMICS A J. Integr. Biol.* **2022**, *26*, 179–188. https://doi.org/10.1089/omi.2021.0227.
7. Konozy, E.H.E.; Osman, M.E.F.M.; Ghartey-Kwansah, G.; et al. The Striking Mimics between COVID-19 and Malaria: A Review. *Front. Immunol.* **2022**, *13*, 957913. https://doi.org/10.3389/fimmu.2022.957913.
8. Sardar, S.; Sharma, R.; Alyamani, T.Y.M.; et al. COVID-19 and Plasmodium Vivax Malaria Co-Infection. *IDCases* **2020**, *21*, e00879. https://doi.org/10.1016/j.idcr.2020.e00879.
9. Hussein, M.I.H.; Albashir, A.A.D.; Elawad, O.A.M.A.; et al. Malaria and COVID-19: Unmasking Their Ties. *Malar. J.* **2020**, *19*, 457. https://doi.org/10.1186/s12936-020-03541-w.
10. Baba, I.A.; Rihan, F.A.; Hincal, E. Analyzing Co-Infection Dynamics: A Mathematical Approach Using Fractional Order Modeling and Laplace-Adomian Decomposition. *J. Biosaf. Biosecur.* **2024**, *6*, 113–124. https://doi.org/10.1016/j.jobb.2024.05.002.
11. Boulaaras, S.; Yavuz, M.; Alrashedi, Y.; et al. Modeling the Co-Dynamics of Vector-Borne Infections with the Application of Optimal Control Theory. *Discret. Contin. Dyn. Syst.-S* **2025**, *18*, 1331–1352. https://doi.org/10.3934/dcdss.2024109.
12. McArdle, A.J.; Turkova, A.; Cunnington, A.J. When Do Co-Infections Matter? *Curr. Opin. Infect. Dis.* **2018**, *31*, 209–215. https://doi.org/10.1097/qco.0000000000000447.
13. Bolaji, B.; Onoja, T.; Agbata, C.; et al. Dynamical Analysis of HIV-TB Co-Infection Transmission Model in the Presence of Treatment for TB. *Bull. Biomath.* **2024**, *2*, 21–56. https://doi.org/10.59292/bulletinbiomath.2024002.
14. Pusparani, A.; Henrina, J.; Cahyadi, A. Co-Infection of COVID-19 and Recurrent Malaria. *J. Infect. Dev. Ctries.* **2021**, *15*, 625–629. https://doi.org/10.3855/jidc.13793.
15. Avusuglo, W.S.; Han, Q.; Woldegerima, W.A.; et al. Assessment of Bidirectional Impact of Stigmatization Induced Self-

Medication on COVID-19 and Malaria Transmissions Using Mathematical Modeling: Nigeria as a Case Study. *Math. Biosci.* **2024**, *376*, 109249. https://doi.org/10.1016/j.mbs.2024.109249.

16. Mahajan, N.N.; Kesarwani, S.N.; Shinde, S.S.; et al. Co-Infection of Malaria and Dengue in Pregnant Women with SARS-CoV-2. *Int. J. Gynecol. Obstet.* **2020**, *151*, 459–462. https://doi.org/10.1002/ijgo.13415.
17. Mohamed, A.H.; Eltyeb, E.; Said, B.; et al. COVID-19 and Malaria Co-Infection: A Systematic Review of Clinical Outcomes in Endemic Areas. *PeerJ* **2024**, *12*, e17160. https://doi.org/10.7717/peerj.17160.
18. López-Farfán, D.; Yerbanga, R.S.; Parres-Mercader, M.; et al. Prevalence of SARS-CoV-2 and Co-Infection with Malaria during the First Wave of the Pandemic (the Burkina Faso Case). *Front. Public Health* **2022**, *10*, 1048404. https://doi.org/10.3389/fpubh.2022.1048404.
19. Carrión-Nessi, F.S.; Mendoza-Millán, D.L.; Omaña-Ávila, Ó.D.; et al. Plasmodium Vivax and SARS-CoV-2 Co-Infection in Venezuelan Pregnant Women: A Case Series. *Malar. J.* **2023**, *22*, 11. https://doi.org/10.1186/s12936-023-04442-4.
20. Abioye, A.I.; Peter, O.J.; Ogunseye, H.A.; et al. Mathematical Model of COVID-19 in Nigeria with Optimal Control. *Results Phys.* **2021**, *28*, 104598. https://doi.org/10.1016/j.rinp.2021.104598.
21. Ayoade, A.A.; Ogunmiloro, O.M.; Oyedepo, T. Analysis of the Effect of Isolation on the Transmission Dynamics of COVID-19: A Mathematical Modelling Approach (R1). *Comput. Methods Differ. Equ.* **2025**, *13*, 123–141. https://doi.org/10.22034/cmde.2024.58127.2451.
22. Bolaji, B.; Odionyenma, U.B.; Omede, B.I.; et al. Modelling the Transmission Dynamics of Omicron Variant of COVID-19 in Densely Populated City of Lagos in Nigeria. *J. Niger. Soc. Phys. Sci.* **2023**, *5*, 1055. https://doi.org/10.46481/jnsps.2023.1055.
23. Iboi, E.A.; Sharomi, O.; Ngonghala, C.N.; et al. Mathematical Modeling and Analysis of COVID-19 Pandemic in Nigeria. *Math. Biosci. Eng.* **2020**, *17*, 7192–7220. https://doi.org/10.3934/mbe.2020369.
24. Ogundokun, R.O.; Lukman, A.F.; Kibria, G.B.M.; et al. Predictive Modelling of COVID-19 Confirmed Cases in Nigeria. *Infect. Dis. Model.* **2020**, *5*, 543–548. https://doi.org/10.1016/j.idm.2020.08.003.
25. Oke, I.I.; Oyebo, Y.T.; Fakoya, O.F.; et al. A Mathematical Model for COVID-19 Disease Transmission Dynamics with Impact of Saturated Treatment: Modeling, Analysis and Simulation. *Open Access Libr. J.* **2021**, *8*, 1–20. https://doi.org/10.4236/oalib.1107332.
26. Ojo, M.M.; Doungmo Goufo, E.F. The Impact of COVID-19 on a Malaria Dominated Region: A Mathematical Analysis and Simulations. *Alex. Eng. J.* **2023**, *65*, 23–39. https://doi.org/10.1016/j.aej.2022.09.045.
27. Ren, Y.; Xue, Y. Modeling and Optimal Control of COVID-19 and Malaria Co-Infection Based on Vaccination. *Math. Model. Control.* **2024**, *4*, 316–335. https://doi.org/10.3934/mmc.2024026.
28. Hu, R.; Aziz, M.H.N.; Mohamed, N.A.; et al. Modeling and Analysis of Dynamical Behavior in a Fractional-Order COVID-19 Epidemic Model with Media Coverage: A Case Study of Malaysia. *Alex. Eng. J.* **2025**, *127*, 1081–1095. https://doi.org/10.1016/j.aej.2025.06.057.
29. Akanni, J.; Ajao, S.; Ayoade, A.A.; et al. Analysis of Fractional-Order Model for COVID-19: Implications for Transmission, Hospitalisation, and Recovery Trends. *Prog. Fract. Differ. Appl.* **2025**, *11*, 467–489. https://doi.org/10.18576/pfda/110304.
30. Abioye, A.I.; Peter, O.J.; Ogunseye, H.A.; et al. A Fractional-Order Mathematical Model for Malaria and COVID-19 Co-Infection Dynamics. *Healthc. Anal.* **2023**, *4*, 100210. https://doi.org/10.1016/j.health.2023.100210.
31. Hu, R.; Aziz, M.H.N.; Aruchunan, E.; et al. Modeling and Analysis of a Delayed Fractional Order COVID-19 SEIHRM Model with Media Coverage in Malaysia. *Sci. Rep.* **2025**, *15*, 25305. https://doi.org/10.1038/s41598-025-99389-8.
32. Chitnis, N.; Hyman, J.M.; Cushing, J.M. Determining Important Parameters in the Spread of Malaria through the Sensitivity Analysis of a Mathematical Model. *Bull. Math. Biol.* **2008**, *70*, 1272–1296. https://doi.org/10.1007/s11538-008-9299-0.
33. Buonomo, B. Analysis of a Malaria Model with Mosquito Host Choice and Bed-Net Control. *Int. J. Biomath.* **2015**, *8*, 1550077. https://doi.org/10.1142/s1793524515500771.
34. Zio, S.; Tougri, I.; Lamien, B. Propagation Du COVID19 Au Burkina Faso, Modelisation Bayesienne Et Quantification Des Incertitudes: Premiere Approche. Available online: https://fr.scribd.com/document/910223015/Covid19-Bf-Modelisation-Numerique-pdf-PDF (accessed on 12 June 2026).
35. Linton, N.M.; Kobayashi, T.; Yang, Y.; et al. Incubation Period and Other Epidemiological Characteristics of 2019 Novel Coronavirus Infections with Right Truncation: A Statistical Analysis of Publicly Available Case Data. *J. Clin. Med.* **2020**, *9*, 538. https://doi.org/10.3390/jcm9020538.
36. Ngonghala, C.N.; Iboi, E.; Eikenberry, S.; et al. Mathematical Assessment of the Impact of Non-Pharmaceutical Interventions on Curtailing the 2019 Novel Coronavirus. *Math. Biosci.* **2020**, *325*, 108364. https://doi.org/10.1016/j.mbs.2020.108364.
37. Tchoumi, S.Y.; Diagne, M.L.; Rwezaura, H.; et al. Malaria and COVID-19 Co-Dynamics: A Mathematical Model and Optimal Control. *Appl. Math. Model.* **2021**, *99*, 294–327. https://doi.org/10.1016/j.apm.2021.06.016.
38. Barley, K.; Murillo, D.; Roudenko, S.; et al. A Mathematical Model of HIV and Malaria Co-Infection in Sub-Saharan Africa. *J. AIDS Clin. Res* **2012**, *3*. https://doi.org/10.4172/2155-6113.1000173.
39. Osman, S.; Makinde, O.D. A Mathematical Model for Coinfection of Listeriosis and Anthrax Diseases. *Int. J. Math. Math. Sci.* **2018**, *2018*, 1–14. https://doi.org/10.1155/2018/1725671.
40. Bonyah, E.; Khan, M.A.; Okosun, K.O.; et al. On the Co-Infection of Dengue Fever and Zika Virus. *Optim. Control. Appl. Methods* **2019**, *40*, 394–421. https://doi.org/10.1002/oca.2483.

41. Van Den Driessche, P.; Watmough, J. Reproduction Numbers and Sub-Threshold Endemic Equilibria for Compartmental Models of Disease Transmission. *Math. Biosci.* **2002**, *180*, 29–48. https://doi.org/10.1016/s0025-5564(02)00108-6.
42. Castillo-Chavev, C.; Feng, Z.; Huang, W. On the Computation of R_0 and Its Role on Global Stability. *Math. Approch. Emerg. Reemerging Infect. Dis.* **2001**, *1*, 25.